

Original Article

Brain Tumor Type Identification from MR Images using Texture Features and Machine Learning Techniques

Jaya H. Dewan^{1*}, Sudeep D. Thepade², Pradnya Deshmukh¹, Sharvari Deshmukh¹, Pooja Katpale¹, Kartik Gandole¹

¹Department of Information Technology, Pimpri Chinchwad College of Engineering, Maharashtra, India.

²Department of Computer Engineering, Pimpri Chinchwad College of Engineering, Maharashtra, India.

^{1*}Corresponding Author : jaya.h.dewan@gmail.com

Received: 23 January 2023

Revised: 17 April 2023

Accepted: 26 April 2023

Published: 25 May 2023

Abstract - Using Magnetic Resonance Imaging (MRI) to find brain tumors is difficult for contemporary medical imaging research. Basically, a brain tumor is an expansion of aberrant brain cells that expand erratically and seemingly uncontrolled. Meningioma, Glioma, and Pituitary are the three kinds of tumors that are most frequently seen. Early identification is essential for the successful treatment of brain tumors. With the development of medical imaging, doctors now employ various imaging methods, such as fMRI, EEG, etc., to diagnose brain tumors. These imaging methods can help clinicians establish a precise diagnosis and create a treatment strategy by providing details on brain tumours' location, size, and shape. Feature extraction and classification are two steps in the categorization of brain tumors. Two traditional manual feature extraction methods were frequently utilized in certain earlier research to extract details like the intensity and texture of images of brain tumors. This work employs the "GLCM (Grey Level Co-occurrence Matrix)" approach for feature extraction. The generated feature set is provided to machine learning (ML) algorithms, including "K-Nearest Neighbors (KNN), Support Vector Machine (SVM), Decision Tree (DT), Naive Bayes (NB), Logistic Regression (LR), Naive Bayes (NB), and Random Forest (RF)". According to experimental results, random forest yields the highest accuracy of 91.04%. The proposed methodology helps classify the different brain tumor classes like glioma, pituitary, meningioma, or no tumor.

Keywords - Brain tumor, Decision tree, GLCM, K-nearest neighbors, Logistic regression, MRI, Naive bayes, Random forest, Support vector machine.

1. Introduction

A brain tumor is the most dangerous type of tumor because it develops fast and disrupts the nervous system's function. A mass of abnormal brain cells is known as a brain tumor. There are several forms of brain tumors; some of them are cancerous (malignant), and others that are not (benign)[1]. Because benign tumors are not usually embedded in brain tissue, they can be readily removed after surgery. However, malignant tumors that begin in the brain grow quicker and have a greater probability of spreading throughout the body, resulting in secondary tumors. Collecting medical image data from various biomedical devices that use several imaging techniques, such as X-ray, CT scan, and MRI, is crucial for diagnosis. A patient's water molecules contain hydrogen atoms, and magnetic field vectors can be detected using radio frequency pulses and high magnetic fields to excite those atoms' nuclei. This technique is known as Magnetic Resonance Imaging (MRI). As compared to CT- Scans, MRI is better for diagnosis as it does not use radiation. Manual evaluation of MRI is the standard approach for identifying brain tumors. However, this is a time-consuming procedure[2]. As a result, Artificial Intelligence may thus help

in the early diagnosis of brain cancers. A large volume of MRI can be analyzed through automated systems as they are the most cost-effective. Also, these automated systems are expected to have high accuracy in dealing with human life. Both supervised and unsupervised algorithms may be applied to categorize brain MR images as abnormal or normal.

This research proposes an effective automated classification methodology for brain MRI using ML methods. Supervised ML algorithms like KNN, SVM, DT, RF, LR and NB are used for brain MR image classification. Feature extraction is done from the input image dataset using the GLCM technique. Feature vectors are formed using GLCM-based statistical features.

The key deliverables of the work presented are:

- Identify the type of brain tumor from MR images using texture features with ML techniques.
- Performance analysis of various GLCM orientations for texture features being used in brain tumor type identification.
- Identification of better-suited ML technique for detecting brain tumor type from MR image.



2. Literature Survey

In this part, prevailing brain tumor detection and categorization techniques are studied. The techniques for pre-processing data and extracting significant features, algorithms for classifying brain tumors, model-building parameters, and the precision of corresponding algorithms in predicting outcomes are analyzed.

Shijin et al.[3] extracted texture characteristics using GLCM while connected regions are used to calculate shape features in the tumor detection system. The pre-processing of the brain MRI includes skull stripping with connected neighbours and morphological techniques. Nine texture characteristics in all are used for the GLCM-based feature extraction. Similar to this, connected regions are used to extract shape attributes utilizing perimeter, area, and circularity. Performance is evaluated using accuracy, recall, and precision. As opposed to current methods, the suggested feature extraction process is simpler and faster.

Q Nida-Ur-Rehman et al.[4] aimed to segment and classify the four most prevalent types of brain tumors. In the proposed model, morphological operations are carried out after pre-processing, and segmentation is done using histogram differencing with a rank filter. KNN is used to categorize photos of cancerous and benign tumors. The TCR rate is determined to be 97.3%, while the FCR rate is determined to be 2.7%.

An ML technique based on the Discrete Wavelet Transform (DWT) is proposed by Keita et al. [5] as a tool for identifying and classifying brain tumours. The kernel SVM classification approach is utilized for training and classification, and features from 2D DWT components are employed to distinguish between benign and malignant MRI images. The proposed method achieves high levels of accuracy, sensitivity, and specificity, around 99%, in identifying brain tumors in MRI images, which is crucial for clinical diagnosis and therapy.

G.Sundari et al.[6] proposed a brain tumor classification system in which pre-processing of the MRI images includes skull stripping, followed by morphological procedures. Methods of deep learning and transfer learning are employed. AlexNet is used to classify the tumor images. Furthermore, GooleNet architecture is used to distinguish malignant and benign images. Accuracy, recall, and precision are utilized to assess performance. An accuracy of about 93.75% is attained.

S. G et al.[7] presented a hybrid ensemble model to categorize brain MRI into two classes: tumor and no tumor. This strategy uses image enhancement as a pre-processing step before morphological processes. In the process of extracting features from the brain tumor, texture and statistical characteristics are computed, and the Local Frequency

Descriptor (LFD) approach is a method to draw out the image's most pronounced features. They are combined to derive hybrid features. In order to categorize the brain MR images, an ensemble classifier is created by incorporating different ML techniques, including SVM, DT, and KNN. This hybrid model has an accuracy rate of 99.8%.

Ullah et al.[8] conducted a rigorous analysis of the various image-processing methods for brain tumor detection. There are many pre-processing techniques used, like denoising, skull stripping, and intensity normalization. It has been shown that the median filter is the optimum method for employing a linear filter. The next process is image enhancement, and here histogram normalization performs best. Additionally, the best system combines independent component analysis, linear discriminant analysis, and PCA(Principal Component Analysis) for feature extraction and feature reduction. Algorithms for supervised learning are evaluated using accuracy, recall, and precision.

Shibu D. S et al. [9]describes the diagnosis of ischemic stroke using CT images and the use of segmentation and feature extraction techniques to differentiate between normal and abnormal brain images. However, traditional segmentation methods may lead to over-segmentation, so the study proposes using Marker-based watershed segmentation to overcome this problem. Statistical and shape features are extracted using grey-level co-occurrence matrix and histogram techniques. To identify brain abnormalities, mathematical computations and comparisons to results from a standard dataset are performed.

A hybrid self-organizing map (SOM) based Fuzzy K Means (FKM) technique that does better pre-processing on MRI is introduced by Vishnuvarthanan et al.[10]. It is more efficient at handling data and also successfully detects the tumor and effectively separates the various tissue regions found inside the brain's tissues. At the initial level, clustering is carried out using SOM. Using FKM, these SOM outcomes are reclustered. Further tissues are segmented, and the tumor is detected. The segmentation findings are validated, and finally, these results assist the surgeon in deciding the radiotherapeutic procedures.

By using ML approaches, T. S. Zignasa et al.[11] can anticipate the tumor's pattern from brain MR scans, which reduces the amount of time and error involved in the procedure. The tumor detection model examines images. CNN is supported for detecting brain tumors and classifying them using MLP. The suggested method combines the neural network technology and entails multiple processes, including system training, pre-processing, tensorflow implementation, and classification.

K. Balasubramanian1 et al.[12] suggested a methodology with four main components - Segmentation, dimensionality

reduction, feature extraction, and classification. The object is first segmented using correlation-based template matching, a versatile high-level ML technique to find the item in complicated templates. Following the application of the Haar Discrete Wavelet Transform (HDWT), hybrid feature extraction (homogeneity and correlation) is carried out on the segmented optic disc image to get feature subsets.

The existing GLCM feature extraction methods calculate the gray-co-matrix for the grey-scale image only. The orientations that are taken into account are also restricted. The proposed methodology analyses model performance for each of the red, green, and blue channels, along with a combination of all channels for various GLCM orientations. ML algorithms are evaluated for their classification performance.

3. Experimental Setup

3.1. Dataset

This study uses data from Kaggle[13]for the analysis. 6935 images from the MRI dataset show the human brain, which falls under the following four categories: glioma (Gl), meningioma (Me), pituitary (Pi), and without tumor (No). The dataset consists of 1599 images of glioma, 1623 images of meningioma, 1735 images of pituitary tumor, and 1978 images of no tumor. The dimensions of every MRI are 512 X 512 X 3 pixels. Figure 1 shows some of the sample MR images. This dataset will be divided into two portions: An estimated 80% of the data is utilized for training, while 20% is used for testing.

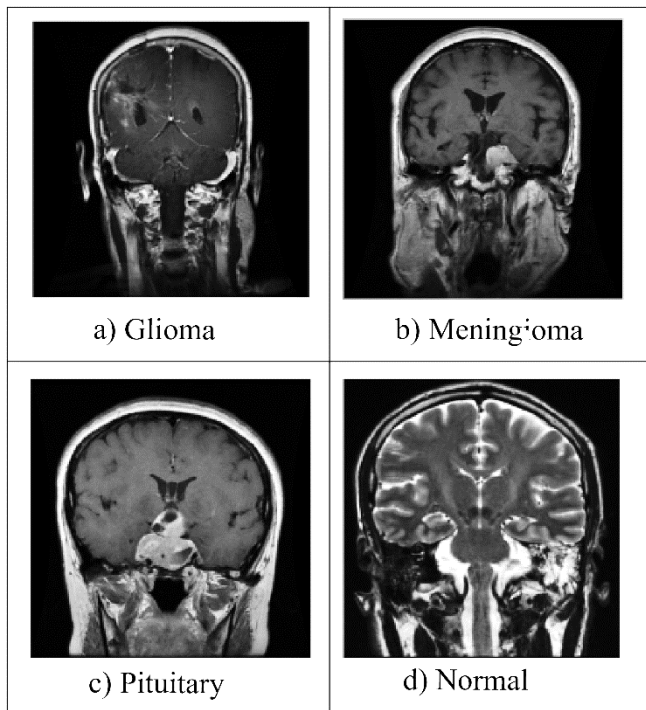


Fig. 1 Sample images from the dataset

3.2. Pre-processing

Pre-processing is necessary for medical image analysis because the noise from imaging devices may degrade the model's performance. Using the Gaussian filter, the picture quality is improved by noise reduction, intensity equalization, and outlier elimination. The 1-D Gaussian distribution has the form shown in Equation.1:

$$G(x) = \frac{1}{\sqrt{2\pi}\sigma} e^{-\frac{x^2}{2\sigma^2}} \tag{1}$$

where σ is the distribution's standard deviation, x, y are the pixel intensities. Additionally, we presupposed that the distribution's mean would be zero. An isotropic (i.e., circularly symmetric) Gaussian in two dimensions has the shape shown in Equation.2:

$$G(x, y) = \frac{1}{\sqrt{2\pi}\sigma^2} e^{-\frac{x^2+y^2}{2\sigma^2}} \tag{2}$$

3.3. Feature Extraction

A crucial stage in computer-aided brain abnormality diagnosis utilizing MRI is feature extraction. A feature is a piece of data about an image's content used in computer vision and image processing to represent the image. It often pertains to whether a certain section of the image possesses particular characteristics. Features in an image can be particular elements like points, edges, or objects[14].

Feature extraction preserves the original data set's information. Compared to using ML on the raw data directly, it produces better outcomes. GLCM is one of the most preferred feature extraction techniques[15].

3.3.1. GLCM-Based Feature Extraction

A GLCM is a statistical technique for texture analysis that accounts for the spatial connection between pixels. The GLCM determines the frequency of pixel pairs to describe an image's texture that occurs with certain values and in a particular spatial relationship. There are four spatial orientations in which co-occurrence matrices can be built: $0^\circ, 45^\circ, 90^\circ, 135^\circ$. Using $N \times N$ as the matrix size and $P(r, t)$ as the matrix of co-occurrence, each element represents the frequency of spatial connections between pixels with grey levels r and t . Figure 2 shows the construction of GLCM from a grey-scale image. The given input image has 10 different grey areas. In different orientations, GLCM depicts the relationship between the neighbouring pixel r and reference pixel t . In this instance, the horizontal and rightward calculation determines the link between the pixels. In the $P(r, t)$, each element's starting value is zero.

Dissimilarity, Correlation, Homogeneity, Contrast, ASM (Angular Second Moment), and Energy are texture properties computed using GLCM [16]. These values are calculated using Equation.3 to Equation.8.

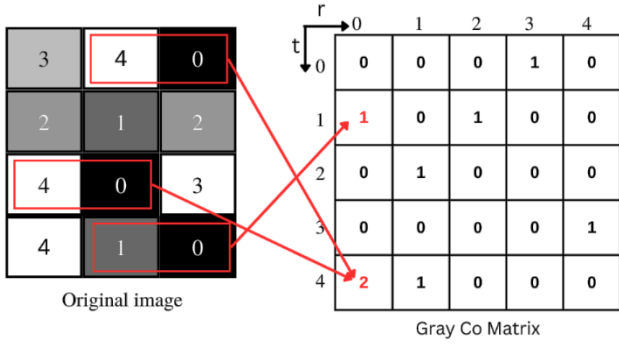


Fig. 2 GLCM technique for gray-co-matrix calculation

Dissimilarity

It calculates the distribution of the image's grey level mean difference. It ranges from 0 to ∞ where 0 specifies pixels are alike, and 1 specifies pixels are dissimilar.

$$Dissimilarity = \sum_{r,t=0}^{N-1} P(r,t)|r-t| \quad (3)$$

Correlation

A pixel's association with its neighboring pixels throughout the whole image is measured by an image's correlation feature. The correlation coefficient ranges from -1 to 1 for fully positive correlated images and is infinite for constant images. μ_r and μ_t represent mean according to r and t references, respectively. σ_r and σ_t represent the standard deviation of values for r and t , respectively.

$$Correlation = \sum_{r,t=0}^{N-1} P(r,t) \left| \frac{(r-\mu_r)(t-\mu_t)}{\sqrt{(\sigma_r^2)(\sigma_t^2)}} \right| \quad (4)$$

Homogeneity

Greater values for lower grey tone differences in a pair of pixels are used to determine image homogeneity. The value for this property lies in the range of 0 to 1.

$$Homogeneity = \sum_{r,t=0}^{N-1} \frac{P(r,t)}{1+(r-t)^2} \quad (5)$$

Contrast

The contrast is a measurement of the intensity of each pixel and its surrounding neighbors. It ranges from 0 to ∞ .

$$Contrast = \sum_{r,t=0}^{N-1} P(r,t)(r-t)^2 \quad (6)$$

Energy

The degree of pixel pair repeats is measured by the energy characteristic. Image texture disorder is measured using energy. This property value lies in the range of 0 to 1. Value 1 for energy is used for the constant image.

$$Energy = \sum_{r,t=0}^{N-1} P(r,t)^2 \quad (7)$$

ASM

It represents the image's grey level distribution for uniformity. It ranges from 0 to 1.

$$ASM = \sum_r \sum_t \{P(r,t)\}^2 \quad (8)$$

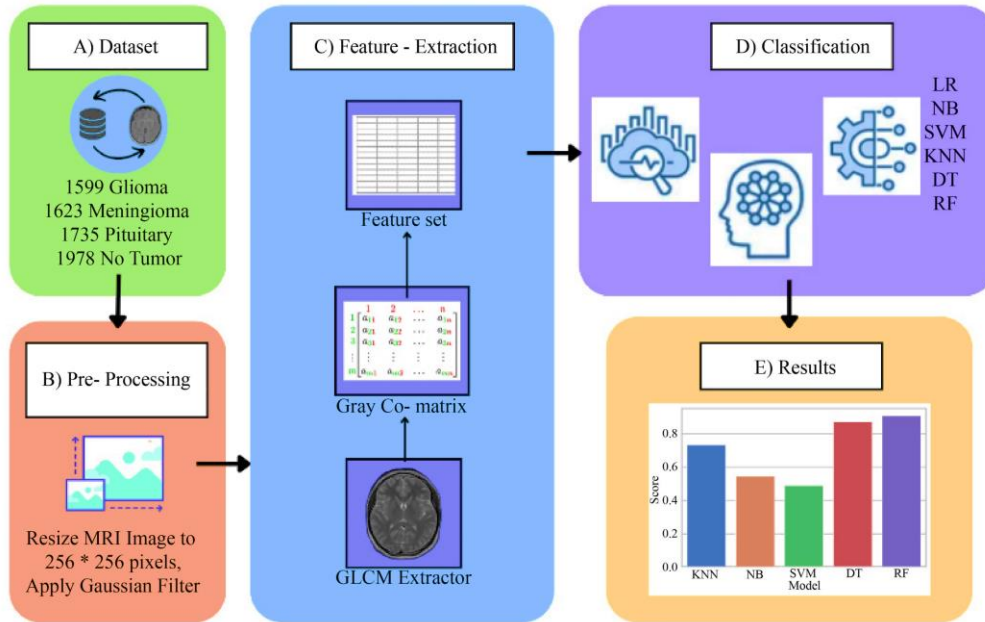


Fig. 3 Proposed methodology for brain tumor type detection

4. Proposed Brain Tumor Type Identification Method

The suggested model of feature extraction based on GLCM and classification employing machine learning techniques is presented in Figure 3. Feature extraction from brain MR images and classification using an ML algorithm are the two main stages of the system. 6935 brain MR images are used in the experiment.

The input image size is (512,512,3) with the tuple parameters specifying height, width, and channel count (RGB). Pixel intensities are in the range of 0 – 255. Various pixel intensity levels that are taken into consideration are 64, 128, and 256. The GLCM matrix is computed for distance as one and selected orientation pairs. In this study, a symmetric gray-co-matrix is generated in which the relationships from r to t and from t to r are identical. According to Figure 4, relative recurrences are calculated for the pair consisting of each pixel and its neighbor. A normalized matrix is created by dividing each element by the sum of all elements in the matrix. The orientations of analysis are:

- 135° : Top left to bottom right
- 90° : Vertical
- 45° : Bottom left to the top right
- 0° : Horizontal

For every image, texture-based features are retrieved. The GLCM features are extracted in two different ways.

4.1. GLCM Feature Extraction using a Single Channel

The red, blue, and green channels are extracted separately from the image. After extracting a specific channel, a symmetric gray-co-matrix is calculated, and the texture features are extracted. This feature set is given to the ML algorithm to build the model. The feature set can be generated in three ways:

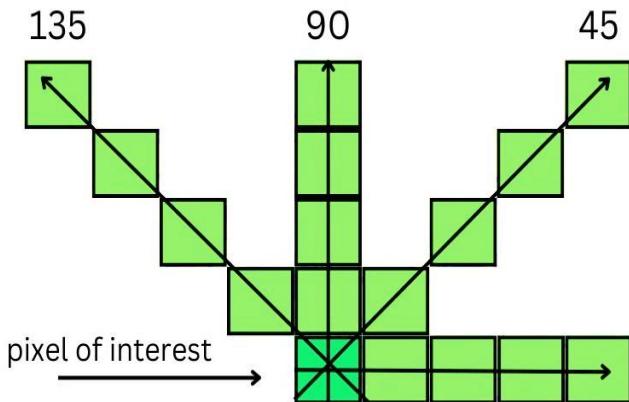


Fig. 4 Various orientations of gray-co-matrix calculation

- By considering all statistical property values for a specific orientation

The feature set is generated by taking into account property values for a specific orientation of a particular channel. Grey-scale image is also considered.

- By considering statistical property values in all orientation

The feature vector is generated by taking into account all the orientations ($0^\circ, 45^\circ, 90^\circ, 135^\circ$) for each of the mentioned properties for a specific channel. So, in this case, the size of the feature vector becomes 6×4 as six texture features are considered here, namely dissimilarity, correlation, homogeneity, contrast, energy and ASM and for all four orientations. Additionally, different grey levels are taken into account (64,128,256) for generating gray level co-occurrence matrix.

- By considering an average of statistical property for all orientations

In this instance, the feature vector is created by averaging a certain attribute across all orientations. As a result, the feature vector is just six parameters in size.

4.2. GLCM Feature Extraction using RGB Channels

The feature vector is generated by considering all the R, G, and B color channels. The feature set can be generated in two ways:

- Fusion of statistical properties using a specific orientation

The feature vector is generated by considering property values for the specific orientation of RGB channels.

- Fusion of average statistical property values using all orientations and RGB channels

The features obtained through all the channels are fused to generate the final feature vector. Here, the average of all the orientations for each attribute is used to create the feature vector for each channel. Thus, the size of the feature vector is 18. Texture-based properties (dissimilarity, homogeneity, energy, contrast, ASM, correlation) are extracted using GLCM. The GLCM features are fed into various ML techniques to build the model. Six machine learning techniques, LR, DT, KNN, NB, SVM, and RF, are considered for comparative analysis.

5. Classification

Different ML methods are explored for the categorization of brain MR images. The whole dataset is separated between training and testing, with 80% for training and the remaining

for testing purposes. Since recall and accuracy are both defined with reference to the positive class, they are utilized in circumstances where performance for the positive class is desirable. With precision, model performance with respect to only relevant data points can be evaluated without including irrelevant data points. F1-score takes into both precision and recall. Performance metrics for each algorithm are recorded, which are accuracy, precision(P), recall(R), and f1-score calculated using Equation.9 to Equation.12, respectively.

$$Accuracy = \frac{TP + TN}{Total\ Samples} \tag{9}$$

$$P = \frac{TP}{TP + FP} \tag{10}$$

$$R = \frac{TP}{TP + FN} \tag{11}$$

$$F1 - score = \frac{2PR}{P + R} \tag{12}$$

Here FP, TN, TP, and FN indicate False Positive, True Negative, True Positive, and False Negative, respectively.

5.1. Support Vector Machine (SVM)[17]

The hyperplane is examined by SVM, which widens the The separation between the classes in the training data. A formulation for a hyperplane is given in Equation.13:

$$f(x) = a^T x + c \tag{13}$$

where, x : input vector, c : bias, a : dimensional coefficient
The ability to choose from a variety of kernels is an advantage of SVM. A considerably more complex structured data set can be used with different kernels. Additionally, it has fewer overfitting issues. Even though the kernel is the SVM's strongest point, choosing a kernel might be challenging. On the other hand, whenever the data set is larger, it requires a lot of computational time.[18]

5.2. Naïve Bayes (NB)[19]

The NB, a widely used method, mathematically adheres to Bayes' theorem. Equation.14 shows the probability calculation using Bayes theorem.

$$P(M|N) = \frac{P(N|M)P(M)}{P(N)} \tag{14}$$

The dependent feature vectors d_i through d_j and the provided class variable e are related, according to the Bayes theorem. Probabilities are computed by the model using Equation.15.

$$P(e|d_i, \dots, d_j) = \frac{P(d_i, \dots, d_j|e)P(e)}{P(d_i, \dots, d_j)} \tag{15}$$

NB requires less computing time as compared to other machine learning algorithms. It can manage category input variables effectively. It assumes each characteristic is an independent variable, making it challenging to use realistically.

5.3. Logistic Regression (LR)[20]

LR is the most popular technique for estimating the likelihood that a certain instance belongs to a particular class (LR). Logistic regression, which derives the log of the dependent variable from the independent variable using the logistic model, identifies the relationship between a categorical result value and one or more predictor values. Equation.16 provides the equation for LR.

$$d = \frac{e^{b_0+b_1c}}{1 + e^{b_0+b_1c}} \tag{16}$$

where,
 c : input value,
 d : value to be predicted,
 b_0 : bias or intercept term,
 b_1 : coefficient for input(c)

The benefit of providing the final classification based on likelihood is offered by LR, nevertheless. Additionally, it may encounter the whole class separation issue.

5.4. K-Nearest Neighbors (KNN)[21]

A technique called KNN looks at K examples of the dataset that are close to the observation. To assess the output of the inspection that should be expected, the procedure will use its output. Euclidean distance is used to determine how far apart two observations are, and Equation.17 denotes the distance between points a and b :

$$d(a_i, b_i) = \sqrt{(a_{i,1} - b_{i,1})^2 + \dots + (a_{i,m} - b_{i,m})^2} \tag{17}$$

Because K closest neighbor does not require initial training and essentially learns from the data set while generating predictions, it uses extremely less computing effort. Due to the fact that it only needs two values:

- (i) The K value and (ii) The distance function value.

However, it has issues when the data set is huge and performs poorly when the data include a lot of dimensions.

5.5. Decision Tree (DT)[22]

The DT algorithm employs a tree-looking model to find potential outcomes, including event outcomes. The target

variables in the tree model can take on a discrete range of values. On the other hand, class labels are denoted by leaves, and branch feature joins in tree structures. Equation.18 is the entropy equation.

$$E = - \sum P(x) \log_2 P(x) \quad (18)$$

where,

E : entropy,

$P(x)$: the probability of a particular outcome (class) of the decision tree

The tree structure, with its varied nodes and edges, is ideally suited for the depiction of the interaction of the variables. When the characteristics undergo monotonic modification, decision trees perform well. However, since decision trees cannot handle linear relationships, they may sometimes become unstable. It becomes exceedingly challenging to grasp the whole decision tree if the terminal nodes are increasingly numerous. The DT method is a branch of RF. Decision trees are characterized by high variance and low bias, and by averaging decision trees, the variance component of the model is decreased. By averaging the prediction, it is feasible to generate unidentified samples.

5.6. Random Forest (RF)[23]

The RF method analyses data using a variety of decision trees, gathering predictions from each one and determining the optimal course of action. It also utilizes the bagging algorithm and an ensemble learning technique that can handle missing value data. With a training set of $A = a_1, \dots$, and responses of $B = b_1, \dots, b_n$, baggingselects a random subset

with substitution of the training set and construct trees to the samples. Aggregating the predictions from each individual tree to provide predictions for unseen samples after training.

6. Experimental Results

As input images have three channels red, green and blue (RGB), the experiment is carried out in two different ways:

6.1. GLCM Feature Extraction using Single Channels

The green, blue and red channels are extracted separately from the image. After extracting a specific channel, a symmetric gray-co-matrix is calculated, and the texture features are extracted. This feature set is given to the ML algorithm in order to build the model. The feature set can be generated in three ways:

6.1.1. By Considering All Statistical Property Values for a Specific Orientation

The model accuracy for each of the orientations for different color channels, along with the gray-scale image, is shown in Table 1. Here each orientation is considered for all the channels separately, and the ML model is trained with the obtained dataset. The NB classifier performs the lowest horizontal orientation performance in red, green and blue channels. The RF classifier has given better performance for vertical orientation in all the channels. The performance of DT and RF classifiers is better in comparison to other classifiers considered. The RF classifier categorizes the tumor classes most efficiently in all the cases. Hence RF is used as a classifier for further analysis.

Table 1. Model Performance by considering a particular orientation for individual channels and grey image

| Channel | Orientation | Accuracy (%) | | | | | |
|---------|-------------|--------------|------|------|-------|-------|-------|
| | | SVM | NB | LR | KNN | DT | RF |
| Grey | 0° | 55.9 | 37.3 | 60.4 | 69.6 | 76.8 | 80.7 |
| | 45° | 59.7 | 44.2 | 62.9 | 68.8 | 75.2 | 79.8 |
| | 90° | 60.9 | 56.8 | 65.9 | 69.9 | 73.2 | 80.3 |
| | 135° | 60.0 | 41.9 | 62.6 | 69.05 | 72.93 | 79.26 |
| Red | 0° | 55.9 | 52.1 | 64.8 | 68.7 | 75.6 | 80.9 |
| | 45° | 49.4 | 54.4 | 67.2 | 68.3 | 73.1 | 78.3 |
| | 90° | 64.5 | 62.7 | 71.2 | 75.08 | 80.4 | 86.1 |
| | 135° | 62.1 | 61.6 | 68.8 | 76.4 | 81.4 | 85.4 |
| Green | 0° | 64.0 | 52.3 | 64.1 | 64.79 | 73.0 | 77.1 |
| | 45° | 64.8 | 52.4 | 69.6 | 68.1 | 75.0 | 80.8 |
| | 90° | 63.7 | 61.6 | 68.9 | 73.5 | 77.1 | 84.4 |
| | 135° | 53.9 | 54.1 | 68.5 | 64.9 | 73.2 | 80.4 |
| Blue | 0° | 52.6 | 53.4 | 66.5 | 67.8 | 75.6 | 78.1 |
| | 45° | 40.1 | 52.5 | 66.9 | 68.2 | 74.5 | 78.6 |
| | 90° | 64.5 | 62.7 | 70.7 | 75.5 | 80.8 | 86.2 |
| | 135° | 46.2 | 52.8 | 66.8 | 65.9 | 73.3 | 78.8 |

Table 2. Model performance for individual channels using different quantization levels

| Channel | Quantization Level | Accuracy (%) |
|---------|--------------------|--------------|
| Red | 64 | 65 |
| | 128 | 64 |
| | 256 | 64.5 |
| Green | 64 | 67.1 |
| | 128 | 64.8 |
| | 256 | 55.8 |
| Blue | 64 | 65.9 |
| | 128 | 67.7 |
| | 256 | 65.3 |

Table 3. Model performance with feature vector generating by considering the average of all orientations for individual channels

| Channel | Accuracy (%) |
|---------|--------------|
| Grey | 79.4 |
| Red | 78.8 |
| Green | 80.6 |
| Blue | 78.5 |

Table 4. Model performance for RGB color channels-based feature vector

| Channel | Orientation | Accuracy (%) |
|---------|------------------------------|--------------|
| RGB | 0° | 89.8 |
| | 45° | 90.0 |
| | 90° | 90.8 |
| | 135° | 89.8 |
| RGB | Avg. of (0°, 45°, 90°, 135°) | 91.04 |

6.1.2. By Considering Statistical Property Values in All Orientation

The feature vector is created by accounting for each of the orientations (0°, 45°, 90°, 135°) for each of the mentioned properties. The results after using such a feature set are shown in Table 2. The feature set built for 256 grey levels shows consistent performance. Hence 256 grey levels are used further to create a grey-co-matrix.

6.1.3. By Considering an Average Of Statistical Property for All Orientations

The feature vector, in this instance, is created by calculating the average attribute across all orientations. As a result, the feature vector is just six parameters in size. The accuracy score is shown in Table 3 for each channel. The average accuracy of the green channel is better than other channels.

6.2. GLCM Feature Extraction using RGB Channels

The final feature vector is created by fusing the features produced via all the channels. Table 4 represents the system performance in terms of accuracy for each orientation and feature vector generated through an average of all the

orientations. Results prove that when the average of all the orientations is considered, the highest classification accuracy of 91.04% is achieved.

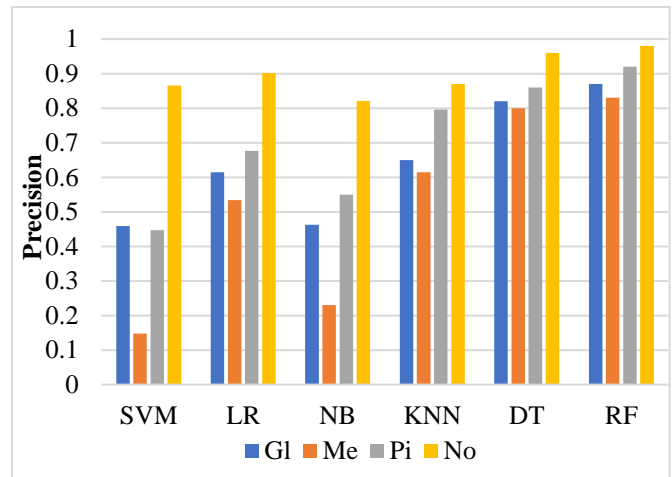


Fig. 5 Precision-based evaluation of the proposed method

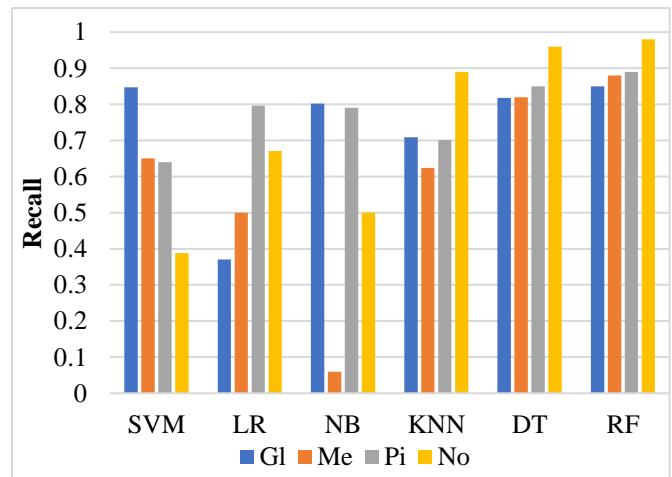


Fig. 6 Recall-based evaluation of the proposed system

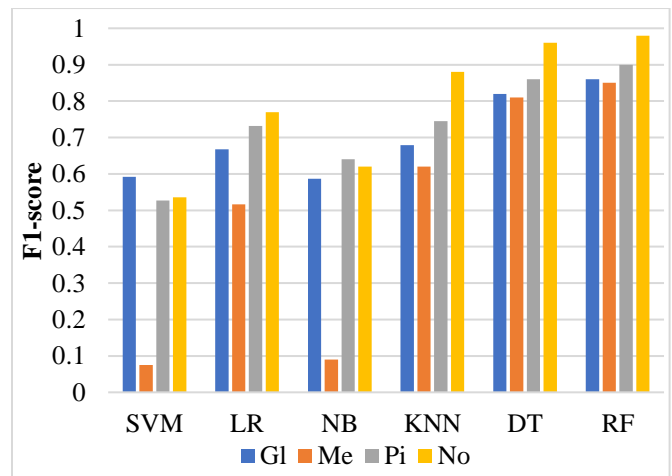


Fig. 7 F1-score-based evaluation of the proposed system

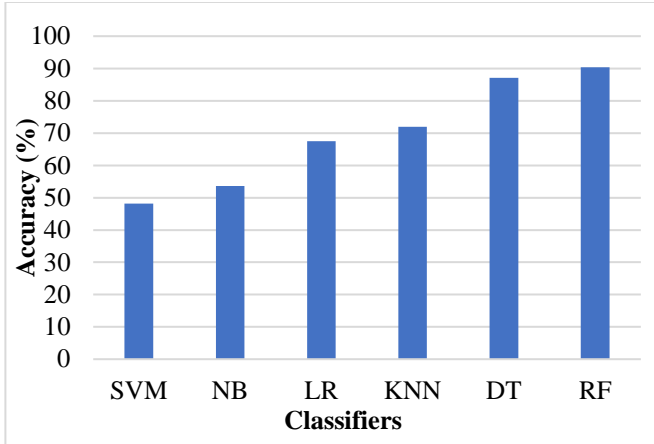


Fig. 8 Performance comparison in terms of accuracy for the proposed GLCM-based model with various classifier

To evaluate the classifiers, a number of widely used metrics are computed. The precision, recall, and f1-score for all the classifiers are shown in Figure 5, Figure 6 and Figure 7, respectively. RF classifier outperformed in all the cases.

References

- [1] Khurram Ejaz et al., "Segmentation Method for Pathological Brain Tumor and Accurate Detection using MRI," *International Journal of Advanced Computer Science and Applications*, vol. 9, no. 8, 2018. [[CrossRef](#)] [[Google Scholar](#)] [[Publisher link](#)]
- [2] Debendra Kumar Sahoo, Satyasis Mishra, and Mihir Narayan Mohanty, "Brain Tumor Segmentation and Classification from MRI Images using Improved FLICM Segmentation and SCA Weight Optimized Wavelet-ELM Model," *International Journal of Advanced Computer Science and Applications*, vol. 13, no. 7, 2022. [[CrossRef](#)] [[Google Scholar](#)] [[Publisher link](#)]
- [3] Shijin Kumar P.S, and Dharun V.S., "Extraction of Texture Features using GLCM and Shape Features using Connected Regions," *International Journal of Engineering and Technology*, vol. 8, no. 6, pp. 2926–2930, 2016. [[CrossRef](#)] [[Google Scholar](#)] [[Publisher link](#)]
- [4] Qazi Nida-Ur-Rehman et al., "Segmentation of Brain Tumor in Multimodal MRI using Histogram Differencing & KNN," *International Journal of Advanced Computer Science and Applications*, vol. 8, no. 4, 2017. [[CrossRef](#)] [[Google Scholar](#)] [[Publisher link](#)]
- [5] Ibrahim Sory Keita et al., "Classification of Benign and Malignant MRIs using SVM Classifier for Brain Tumor Detection," *International Journal of Engineering Trends and Technology*, vol. 70, no. 2, pp. 230–240, 2022. [[CrossRef](#)] [[Publisher link](#)]
- [6] Sunita M. Kulkarni, and G. Sundari, "A Framework for Brain Tumor Segmentation and Classification using Deep Learning Algorithm," *International Journal of Advanced Computer Science and Applications*, vol. 11, no. 8, 2020. [[CrossRef](#)] [[Google Scholar](#)] [[Publisher link](#)]
- [7] G. Shruthi, and Krishna Raj P. M, "Local Frequency Descriptor and Hybrid Features for Classification of Brain Magnetic Resonance Images using Ensemble Classifier," *International Journal of Advanced Computer Science and Applications*, vol. 12, no. 11, 2021. [[CrossRef](#)] [[Google Scholar](#)] [[Publisher link](#)]
- [8] Zahid Ullah, Su-Hyun Lee, and Donghyeok An, "Critical Analysis of Brain Magnetic Resonance Images Tumor Detection and Classification Techniques," *International Journal of Advanced Computer Science and Applications*, vol. 11, no. 1, 2020. [[CrossRef](#)] [[Google Scholar](#)] [[Publisher link](#)]
- [9] S. Pavithra, S. Sivasankari, and D. Sunderlin Shibu, "Hybrid Segmentation and Features Extraction of Ischemic Stroke on CT Brain," *International Journal of Engineering Trends and Technology*, vol. 42, no. 3, pp. 96–101, 2016. [[CrossRef](#)] [[Publisher link](#)]
- [10] G. Vishnuvarthanan et al., "An Unsupervised Learning Method with a Clustering Approach for Tumor Identification and Tissue Segmentation in Magnetic Resonance Brain Images," *Applied Soft Computing*, vol. 38, pp. 190–212, 2016. [[CrossRef](#)] [[Google Scholar](#)] [[Publisher link](#)]
- [11] Tumuluru Sai Zignasa et al., "Brain Tumor Detection Using Machine Learning," *International Journal of Engineering Applied Sciences and Technology*, vol. 6, no. 8, pp. 221–225, 2021. [[CrossRef](#)]
- [12] Kishore Balasubramanian, N. P. Ananthamoorthy, and K. Gayathridevi, "Automatic Diagnosis and Classification of Glaucoma Using Hybrid Features and k -Nearest Neighbor," *Journal of Medical Imaging and Health Informatics*, vol. 8, no. 8, pp. 1598–1606, 2018. [[CrossRef](#)] [[Google Scholar](#)] [[Publisher link](#)]
- [13] Msoud Nickparvar, "Brain Tumor MRI Dataset,"

From the analysis, it is clear that the combined feature vector of texture properties from RGB color planes with an average of all the orientations for each property is the most suitable feature set to be used for the classification.

7. Conclusion

The suggested approach for brain tumor detection in this research makes use of texture-based characteristics derived from GLCM with all the symmetric orientations and classification using ML techniques.

This suggested work considers the image's energy, contrast, correlation, homogeneity, ASM, and dissimilarity as texture aspects. SVM, KNN, NB, LR, DT, and RF ML algorithms are utilized for categorization. The fusion of texture characteristics from RGB color planes by averaging out all the orientations for each property with 256 grey levels yields the highest accuracy of 91.04% when classification is done using RF classifier on the brain MR image dataset from Kaggle. Random forest outperformed in all the performance metrics like precision, recall, f1-score and accuracy.

- [14] Jaya H. Dewan, and Sudeep D. Thepade, "Fusion based Image Retrieval using Haralick Moments and TSBTC Features," *2021 International Conference on Emerging Smart Computing and Informatics (ESCI)*, 2021. [[CrossRef](#)] [[Google Scholar](#)] [[Publisher link](#)]
- [15] Jaya H. Dewan, and Sudeep D. Thepade, "Image Retrieval using Weighted Fusion of GLCM and TSBTC Features," *2021 6th International Conference for Convergence in Technology (I2CT)*, 2021. [[CrossRef](#)] [[Google Scholar](#)] [[Publisher link](#)]
- [16] R. M. Haralick, "Statistical and Structural Approaches to Texture," *Proceedings of the IEEE*, vol. 67, no. 5, pp. 786–804, 1979. [[CrossRef](#)] [[Google Scholar](#)] [[Publisher link](#)]
- [17] Ahmed Hamza Osman, and Hani Moetque Aljahdali, "Diabetes Disease Diagnosis Method based on Feature Extraction using K-SVM," *International Journal of Advanced Computer Science and Applications*, vol. 8, no. 1, 2017. [[CrossRef](#)] [[Google Scholar](#)] [[Publisher link](#)]
- [18] Xuemei Yao, "Application of Optimized SVM in Sample Classification," *International Journal of Advanced Computer Science and Applications*, vol. 13, no. 6, 2022. [[CrossRef](#)] [[Google Scholar](#)] [[Publisher link](#)]
- [19] Ahmad Ashari, Iman Paryudi, and A. Min Tjoa, "Performance Comparison between Naïve Bayes, Decision Tree and k-Nearest Neighbor in Searching Alternative Design in an Energy Simulation Tool," *International Journal of Advanced Computer Science and Applications*, vol. 4, no. 11, 2013. [[CrossRef](#)] [[Google Scholar](#)] [[Publisher link](#)]
- [20] Muhammad Umar Khan et al., "Classification of EMG Signals for Assessment of Neuromuscular Disorder using Empirical Mode Decomposition and Logistic Regression," *2019 International Conference on Applied and Engineering Mathematics (ICAEM)*, 2019. [[CrossRef](#)] [[Google Scholar](#)] [[Publisher link](#)]
- [21] Xueying Zhang, and Qinbao Song, "Predicting the Number of Nearest Neighbors for the k-NN Classification Algorithm," *Intelligent Data Analysis*, vol. 18, no. 3, pp. 449–464, 2014. [[CrossRef](#)] [[Google Scholar](#)] [[Publisher link](#)]
- [22] Mohammad M. Ghiasi, Sohrab Zendejboudi, and Ali Asghar Mohsenipour, "Decision Tree-based Diagnosis of Coronary Artery Disease: CART Model," *Computer Methods and Programs in Biomedicine*, vol. 192, p. 105400, 2020. [[CrossRef](#)] [[Google Scholar](#)] [[Publisher link](#)]
- [23] Yanli Liu, Yourong Wang, and Jian Zhang, "New Machine Learning Algorithm: Random Forest," *Information Computing and Applications*, pp. 246–252, 2012. [[CrossRef](#)] [[Google Scholar](#)] [[Publisher link](#)]
- [24] R. Tamilaruvi et al., "Brain Tumor Detection in MRI Images using Convolutional Neural Network Technique," *SSRG International Journal of Electrical and Electronics Engineering*, vol. 9, no. 12, pp. 198-208, 2022. [[CrossRef](#)] [[Publisher link](#)]
- [25] Sindhia et al., "Brain Tumor Detection Using MRI by Classification and Segmentation," *SSRG International Journal of Medical Science*, vol. 6, no. 3, pp. 12-14, 2019. [[CrossRef](#)] [[Publisher link](#)]
- [26] V. Vinay Kumar, and P. Grace Kanmani Prince, "Gaussian Weighted Deep CNN with LSTM for Brain Tumor Detection," *SSRG International Journal of Electrical and Electronics Engineering*, vol. 10, no. 1, pp. 197-208, 2023. [[CrossRef](#)] [[Publisher link](#)]
- [27] R. Sakthi Prabha, and M. Vadivel, "Brain Tumor Stages Prediction using FMS-DLNN Classifier and Automatic RPO-RG Segmentation," *SSRG International Journal of Electrical and Electronics Engineering*, vol. 10, no. 2, pp. 110-121, 2023. [[CrossRef](#)] [[Publisher link](#)]